Journal of Proteomics 208 (2019) 103470

Contents lists available at ScienceDirect

Journal of Proteomics

journal homepage: www.elsevier.com/locate/jprot

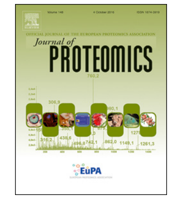


# Integrative omics of *Lonicera japonica* Thunb. Flower development unravels molecular changes regulating secondary metabolites

Bingxian Yang[a], Zhuoheng Zhong[b], Tantan Wang[b], Yuting Ou[b], Jingkui Tian[b], Setsuko Komatsu[c], Lin Zhang[a,*]

[a] *College of Life Science, Zhejiang Sci-Tech University, Hangzhou 310018, China*
[b] *College of Biomedical Engineering & Instrument Science, Zhejiang University, Hangzhou 310027, China*
[c] *Faculty of Environmental and Information Sciences, Fukui University of Technology, Fukui 910-8505, Japan*

ARTICLE INFO

*Keywords:*
*Lonicera japonica* Thunb.
Omics
Flower development
Flavonoids
Terpenoids

ABSTRACT

*Lonicera japonica* Thunb. is an important medicinal plant. The secondary metabolites in L. *japonica* are diverse and vary in levels during development, leading to the ambiguous evaluation for its medical value. In order to reveal the regulatory mechanism of secondary metabolites during the flowering stages, transcriptomic, proteomic, and metabolomic analyses were performed. The integration analysis of omic-data illustrated that the metabolic changes over the flower developmental stages were mainly involved in sugar metabolism, lipopolysaccharide biosynthesis, carbon conversion, and secondary metabolism. Further proteomic analysis revealed that uniquely identified proteins were mainly involved in glycolysis/phenylpropanoids and tricarboxylic acid cycle/terpenoid backbone pathways in early and late stages, respectively. Transketolase was commonly identified in the 5 developmental stages and 2-fold increase in gold flowering stage compared with juvenile bud stage. Simple phenylpropanoids/flavonoids and 1-deoxy-D-xylulose-5-phosphate were accumulated in early stages and upregulated in late stages, respectively. These results indicate that phenylpropanoids were accumulated attributing to the activated glycolysis process in the early stages, while the terpenoids biosynthetic pathways might be promoted by the transketolase-contained regulatory circuit in the late stages of L. *japonica* flower development.

*Biological Significance: Lonicera japonica* Thunb. is a native species in the East Asian and used in traditional Chinese medicine. In order to reveal the regulatory mechanism of secondary metabolites during the flowering stages, transcriptomic, proteomic, and metabolomic analyses were performed. The integration analysis of omic-data illustrated that the metabolic changes over the flower developmental stages were mainly involved in sugar metabolism, lipopolysaccharide biosynthesis, carbon conversion, and secondary metabolism. Our results indicate that phenylpropanoids were accumulated attributing to the activated glycolysis process in the early stages, while the terpenoids biosynthetic pathways might be promoted by the transketolase-contained regulatory circuit in the late stages of L. *japonica* flower development.

## 1. Introduction

*Lonicera japonica* Thunb., a native species of the Eastern Asia, is used in traditional Chinese medicine for thousands of years [1]. Pharmacological studies have demonstrated that L. *japonica* flower possesses antibacterial [2], anti-inflammatory [3], and antiviral [4] and various other pharmacological effects. The flower is also used for prevention and treatment of severe acute respiratory syndromes, H1N1

*Abbreviations:* LJF, *L. japonica* flower; JBS, juvenile bud stage; TGS, third green stage; CWS, complete white stage; SFS, silver flowering stage; GFS, gold flowering stage; TCA, tricarboxylic acid; GC, gas chromatography; TOF, time-of-flight; KEGG, Kyoto Encyclopedia of Genes and Genomes; PCA, principal component analysis; PK, pyruvate kinase; MPDM, 2-methyl-6-phytyl-1,4-hydroquinone methyltransferase; DXPPRI, 1-deoxy-D-xylulose 5-phosphate reductoisomerase; FBPA, fructose-bisphosphate aldolase; PGK, phosphoglycerate kinase; GAPD, glyceraldehyde-3-phosphate dehydrogenase; GGPS, geranylgeranyl pyrophosphate synthase; NDME, NAD-dependent malic enzyme 2; MDH, malate dehydrogenase; CST, citrate synthase; PDGC, pyruvate dehydrogenase E1 component subunit alpha; HMCR, 3-hydroxy-3-methylglutaryl-coenzyme A reductase; CHS, chalcone synthase; 4CL, 4-coumarate–CoA ligase; DAP, differentially abundant protein; cDAPs, commonly identified DAPs; FA, fatty acid; fad, fatty acid desaturase; JA, jasmonic acid; LA, linolenic acid; TK, transketolase; MEP, methylerythritol pathway; G3P, glyceraldehyde 3-phosphate; DXPS, 1-deoxy-D-xylulose-5-phosphate; TPP, thiamine pyrophosphate; AAT, alanine aminotransferase.

* Corresponding author.
*E-mail address:* zhanglin@zju.edu.cn (L. Zhang).

https://doi.org/10.1016/j.jprot.2019.103470
Received 23 January 2019; Received in revised form 12 July 2019; Accepted 24 July 2019
Available online 30 July 2019

influenza, and hand-foot-and-mouth disease [5]. The quality of L. *japonica* mainly depends on the developmental period of the flower. The content of chlorogenic acid which is an important active ingredient [6] is high during early stages while it decreased during late stages of flower development [7]. The flowering period, from May to September, can be divided into five stages according to previous publication [8]: the juvenile bud stage (JBS), the third green stage (TGS), the complete white stage (CWS), the silver flowering stage (SFS), and the gold flowering stage (GFS). A deep explanation for content change of active ingredients during flower development of L. *japonica* has been not performed.

Flowering time is controlled by different pathways, including photoperiod, gibberellin, autonomous, and vernalization [9]. These multiple floral-promoting signals regulated the expression of common set of genes leading to changes in cellular metabolism [10]. The regulation analysis of carbohydrate metabolism [11], pigment biosynthesis and volatile scent compounds during flower development have been performed. The difference of carotenoids content during the flower petal development of marigold were explained by expression analysis of relative genes [12]. The level of transcripts and metabolites was harmonically up-regulated during scent and petal development [13]. The flower contains phenolics, flavonoids, and iridoid glycosides due to which it is the main organ with pharmacological activity [14]. As the chemical compounds show diversification in L. *japonica* and its related species, a systemic analysis is needed to reveal the regulatory mechanisms of the metabolic network during the floral development. Interactive biochemical networks [15], constituting co-regulation of transcripts, proteins, and metabolites results in physiological adjustments of the plant development. A systems biology approach based on omics technology can reconstruct these 'interactive biochemical networks' and help in identifying the interactions that exist between its components. An integrative analysis of transcriptome and metabolome has revealed the links betweenγ-aminobutyric acid signaling, tricarboxylic acid (TCA) cycle status/inositol phosphates, and jasmonate signaling in sensitive/tolerant rice cultivars under high night temperature stress [16]. A systemic approach provided new insights into complex post-transcriptional and translational hierarchies that govern crassulacean acid metabolism in Agave [17]. AGAMOUS-LIKE 22 (AGL22) was identified as a key hub gene in gene regulatory networks in *Arabidopsis* that linked changes in primary metabolism with the initiation of stress responses [18].

In *Catharanthus roseus* the correlation between hormone metabolism and indole alkaloid biosynthesis was revealed through gene-to-gene and gene-to-metabolite networks [19]. Furthermore, Kim et al. [20] revealed the patterns of metabolic changes from large-scale gene regulations and relationships between these regulated genes and metabolic changes. Although secondary metabolites possess important role in normal plant growth and development [21], the enormous biosynthetic potential of secondary metabolites in plant cells still remains unexploited.

It was revealed that the gene families involved in phenylpropanoid biosynthesis and other chemical compounds show diversification in L. *japonica* and its related species including L. *hypoglauca*, *L. macranthoides*, and L. *confusa* [22–23]. Because of non-determinacy, the medicinal value of L. *japonica* and its related species has been quite underestimated. A system biology approach can highlight the potential of extensive metabolic profiling in order to obtain deeper insights into secondary metabolites biosynthesis.

In order to maximize the medicinal value and offer an opportunity to commercially produce plants with increased health benefits, a systemic understanding of the metabolic networks during the floral development is urgently needed. In this study, transcriptomics, proteomics, and metabolomics were performed to construct metabolic network for mining temporal reprogramming of metabolism in L. *japonica*. UPLC TOF-MSMS and qRT-PCR technologies were used for the confirmation of functional predication of identified genes, metabolites, and proteins. This approach can highlight the inherent value in using broad metabolic profiling to understand the regulation of molecular events and help to get deeper insight into secondary metabolites biosynthesis.

## 2. Material and methods

### 2.1. Plant material and growth conditions

*L. japonica* plants were grown in different fields of Pingyi cultivation base (Shandong, China) under controlled conditions. *L. japonica* flowers presented different developmental stages (JBS, TGS, CWS, SFS, and GFS) on same plant during late May. Flowers in the 5 developmental stages were collected respectively. Flowers of same developmental stage from at least ten plants were mixed as one biological replicate. Three and six independent experiments were performed as biological replicates for transcriptomic/proteomic and metabolomic experiments, respectively. Collected plant materials were frozen in liquid nitrogen and stored at −80 °C for the further analysis.

### 2.2. Protein extraction, enrichment, and digestion for proteomics

A portion (50 mg) of each sample was ground to powder in liquid nitrogen using a mortar and pestle. The powder was added to an acetone solution containing 10% trichloroacetic acid and 0.07% 2-mercaptoethanol [24]. The resulting mixture was vortexed and sonicated for 10 min. The suspension was incubated for 1 h at −20 °C with vortexing every 15 min and then centrifuged at 9000 x*g* for 20 min at 4 °C. The pellet was washed twice with 0.07% 2-mercaptoethanol in acetone, dried using a Speed-Vac concentrator (Savant Instruments, Hickville, NY, USA), and resuspended in lysis buffer consisting of 7 M urea, 2 M thiourea, 5% CHAPS, and 2 mM tributylphosphine by vortexing for 1 h at 25 °C. The resulting suspension was centrifuged at 20,000 x*g* for 20 min at 25 °C and the supernatant was collected as crude extract. Protein concentrations were determined using the Bradford assay [25] with bovine serum albumin as the standard.

Proteins (100 μg) were cleaned up with methanol and chloroform to remove any detergent from the sample solutions [26]. About 400 μL of methanol was added and mixed before the further addition of 100 μL of chloroform and 300 μL of water. After mixing, the samples were centrifuged at 20,000 x*g* for 10 min to achieve phase separation. The upper aqueous phase was discarded and 300 μL of methanol was added slowly to lower phase. The samples were centrifuged at 20,000 ×*g* for 10 min and the pellets were dried. These dried pellets were resuspended in 50 mM $NH_4HCO_3$, reduced with 50 mM dithiothreitol for 30 min at 56 °C and alkylated with 50 mM iodoacetamide for 30 min at 37 °C in the dark. Alkylated proteins were digested with trypsin and lysyl endopeptidase (Wako, Osaka, Japan) at 1:100 enzyme/protein (*w*/w) concentrations at 37 °C for 16 h. The resulting tryptic peptides were acidified by formic acid (pH < 3), and centrifuged at 20,000 x*g* for 10 min. The obtained supernatant was collected for the following analysis.

### 2.3. Nanoliquid chromatography-tandem mass spectrometry analysis

Peptides in 0.1% formic acid were loaded onto an Ultimate 3000 nanoLC system (Dionex, Germering, Germany) equipped with a C18 PepMap trap column (300 μm ID x 5 mm; Dionex). Peptides were eluted from the trap column and separated using 0.1% formic acid in acetonitrile at a flow rate of 200 nL/min on a C18 Tip column (75 μm ID x 120 mm; Nikkyo Technos, Tokyo, Japan) with a spray voltage of 1.8 kV. Peptide ions were analyzed on a nanospray LTQ Orbitrap MS (Thermo Fisher Scientific, San Jose, CA, USA) operated in data-dependent acquisition mode with the installed Xcalibur software (version 2.1; Thermo Fisher Scientific). Full-scan mass spectra were acquired in the LTQ Orbitrap MS over 400–1500 *m/z* with a resolution of 30,000. A lock mass function was used to obtain high mass accuracy [27]. As the lock mass, the ions $C_{24}H_{39}O_4{}^+$ (*m/z* 391.28429), $C_{14}H_{46}NO_7Si_7{}^+$ (*m/z* 536.16536), and $C_{16}H_{52}NO_8Si_8{}^+$ (*m/z* 610.18416) were used. Values for ion isolation window were set as follows: activation type was collision-induced dissociation, default charge state was 2, isolation width was 2.0 *m/z*, normalized collision energy was 35%, and activation time was 30 ms. Values for dynamic exclusion were determined as follows: repeat count was 2, repeat duration was 30 s, exclusion list size was 500 m *sec*, exclusion duration was 90 s, and exclusion mass width was ± 1.5 Da. The ten most intense precursor ions above a threshold value of 500 were selected for collision-induced fragmentation. The acquired MS/MS spectra were used for protein identification.

### 2.4. Protein identification from the mass spectrometry data

Proteins were identified using the Mascot search engine (version 2.5.1; Matrix Science, London, UK) with UniProtKB/Swiss-Prot database (Release 2016_02, 550,552 sequences, http://www.uniprot.org/uniprot/). DTA files were generated from acquired raw data files and then converted to Mascot generic files using Proteome Discoverer software (version 1.4.0.288; Thermo Fisher Scientific). The parameters used in the Mascot searches were as follows: carbamidomethylation of cysteine was set as a fixed modification and oxidation of methionine was set as a variable modification. Trypsin was specified as the proteolytic enzyme and one missed cleavage was allowed. Peptide mass tolerance was set at 10 ppm, fragment mass tolerance was set at 0.8 Da, and peptide charges were set at +2, +3, and + 4. An automatic decoy database search was performed as part of the search. Mascot results were filtered with the Mascot percolator to improve the accuracy and sensitivity of peptide identification [28]. False discovery rates for peptide identification of all searches were < 1.0%. Peptides with a percolator ion score of > 13 and a *p*-value < .05 were used for protein identification. The minimum requirement for the identification of a protein was two matched peptides and a *p* value < .05. Proteins identified in all biological replicates were used in this experiment. Proteins with the most significantly matched peptides were saved when peptides were common among different isoforms. Protein abundance was analyzed based on the emPAI value [29]. The mean of three emPAI values was divided by the sum of the emPAI values for all identified protein and multiplied by 100. Protein content was estimated by the molar fraction percentage (mol%).

### 2.5. RNA extraction for transcriptomics

A portion (100 mg) of each sample was ground to powder in liquid nitrogen using a mortar and pestle. Total RNA was isolated using RNeasy Plant Mini kit (Qiagen, Hilden, Germany). The quantity and quality were determined using Agilent 2100 Bioanalyzer (Agilent Technologies, Palo Alto, CA, USA). The poly (A) mRNA was isolated from total RNA samples with Magnetic Oligo (dT) Beads (Illumina, San Diego, CA, USA) and used for mRNA-Sequencing library construction. cDNA was synthesized using the fragmented mRNA and end-repaired followed by a single 'A' base addition. mRNA-Sequencing Sample Preparation Kit (Illumina) was used to prepare the DNA fragments for ligation to the adapters. After purification, the cDNA fragments (200 ± 25 bp) were excised and retrieved. PCR was performed to selectively enrich and amplify the cDNA fragments. Libraries were prepared from a 150–200 bp size-selected fraction following adapter ligation and agarose gel separation.

### 2.6. Transcriptomic sequencing, data processing, and expression analysis of genes

The quality control analysis of the sample libraries was performed. After validation with a Mastercycler ep realplex Real-time PCR System (Eppendorf, Hamburg, Germany), the mRNA-sequencing libraries were sequenced using a paired end read protocol with 100 base pairs of data collected per run on the Hiseq 2000 sequencing platform (Illumina). *De novo* assembly of the transcripts was carried out using the short-read assembly program 'Trinity' [30–31]. Unigene sequences were aligned by BLASTX to UniProtKB/Swiss-Prot database using an *E*-value cut-off of $10^{-5}$. Coding sequence regions were determined for the highest-ranked proteins using BLAST. Unigenes that could not be aligned to database were scanned by ESTScan [32] to determine the nucleotide (5′–3′) and amino acid sequences of the coding regions. The value of fragments per kilobase of exon million fragments mapped was used to represent the expression level of genes.

### 2.7. Metabolite extraction and gas chromatography time-of-flight mass spectrometry analysis

A portion (40 mg) of each freeze-dried sample was added to 0.5 mL of 75% methanol containing adonitol (Sigma, St. Louis, MO, USA) as an internal standard. The resulting mixture was vortexed for 10 s and homogenized using a ball mill for 3 min at 65 Hz. After centrifugation at 12,000 xg for 15 min at 4 °C, the obtained supernatant was used as metabolite extract. A quality control sample was prepared by mixing equal volumes of all extracts. The extract and control samples were dried using a vacuum concentrator, resuspended in 80 μL of methoxylamine hydrochloride, and incubated for 20 min at 80 °C. Subsequently, 100 μL of *N*-methyl-bis-trifluoroacetamide containing 1% trimethylchlorosilane was added to each sample, followed by further incubation for 1 h at 70 °C. The samples were cooled to room temperature, mixed with 10 μL of standard fatty acid methyl esters, and then analyzed by gas chromatography (GC) time-of-flight (TOF)/MS.

GC-TOF/MS analysis was performed on a 7890 GC system (Agilent Technologies, Palo Alto, CA, USA) coupled with a Pegasus HT TOF/MS (LECO, St Joseph, MI, USA) and a Rxi-5Sil MS column (250 μm ID x 30 m; Restek, Bellefonte, PA, USA). Samples (1 μL aliquots) were injected into the splitless injector at 280 °C in split mode. The front inlet purge flow was 3 mL $min^{-1}$ and the gas flow rate through the column was 20 mL $min^{-1}$. After keeping at 50 °C for 1 min, the temperature was raised to 330 °C at a rate of 10 °C $min^{-1}$ and kept for 5 min. The ion source was held at 220 °C the energy was −70 eV in electron impact mode. After 366 s of solvent delay, the detector was used in full scan mode (50–800 *m/z*). All samples were measured in a randomized manner. Raw peaks were identified using ChromaTOF software (version 4.3×; LECO) and the LECO-Fiehn Rtx5 database (version Rtx5; LECO). The retention time index method was used for peak identification with a retention time tolerance of 5000. For quantification of metabolites, peaks were left through interquartile range denoising method. The missing values of raw data were filled up by half of the minimum value. Total area of each sample integration area was normalized for each sample. Based on this method, stable and reliable raw data were achieved for metabolomics analysis.

### 2.8. Secondary metabolites analyses

A portion (300 mg) of each freeze-dried sample was added to 3 mL methanol and the resulting mixture was sonicated for 1 h at 4 °C. The suspension was centrifuged at 10,000 ×*g* for 10 min at 4 °C and the obtained supernatant was filtered through a syringe-driven filter (0.45 μm). The filtrate was dried in a vacuum concentrator, re-dissolved in 100 μL methanol, and used as metabolite extract. Three biological replicates were performed and each biological replicate was technically duplicated to reduce the error rate [33].

The metabolite samples were analyzed on a Triple-TOF 5600 System (AB Sciex, Framingham, MA, USA) fitted with a DuoSpray ion source (AB Sciex) which was connected to an LC system. The separation of all samples was performed on a C18 column (2.1 mm ID x 100 mm, Waters, Dublin, Ireland) with a column temperature at 40 °C. The flow rate was 1 mL $min^{-1}$, and the mobile phase consisted of 0.1% formic acid aqueous and acetonitrile: 0–10 min (8% acetonitrile), 11–20 min (13.6% acetonitrile), 21–30 min (15.2% acetonitrile), 31–60 min (19.2% acetonitrile), 61–80 min (47.2% acetonitrile), and 81–90 min (95% acetonitrile). The sample injection volume was 2 μL. The source voltage and temperature were set to 4500 V and 550 °C for negative ionization mode. The de-clustering potential was 100 V and the collision energy was 35 ± 10 eV. The curtain gas flow was set to 30 arbitrary units and the ion source gas pressure was 50 psi. The mass range was 50–1000 *m/z*. The accumulation time was set at 0.15 s for MS analysis and 0.08 s for MS/MS analysis. Acquisition of the MS/MS spectra was controlled by the information-dependent acquisition (IDA) function of Analyst TF software (version 1.5.1; AB Sciex). Mass accuracy was maintained by use of an automated calibrant delivery system (AB Sciex) interfaced to the second inlet of the DuoSpray source. The calibrant delivery system was set to be an external calibration for each sample. Total sum area module was used for total ion chromatogram normalization and the normalized intensities were integrated for each sample. The data processing was performed using PeakView software (version 1.1, AB Sciex) and MS/MS libraries (Chemspider, http://www.chemspider.com; Metlin, http://metlin.scripps.edu/xcms/; HMDB, http://www.hmdb.ca/).

### 2.9. qRT-PCR analysis

Flower samples of L. *japonica* were collected from each of the five developmental stages separately. A portion (100 mg) of each sample was ground to powder in liquid nitrogen using a mortar and pestle. Total RNA was isolated using the method described above. RNA was reverse-transcribed using a cDNA synthesis kit (Promega, Madison, WI, USA) according to the manufacturer's instructions. The qRT-PCR was performed using an EvaGreen qPCR MasterMix (Applied Biological Materials, Richmond, BC, Canada) on a MyiQ2 two-color real-time PCR detection system (Bio-Rad, Hercules, CA, USA). The reaction conditions were as follows: 95 °C for 600 s followed by 35 cycles of 95 °C for 15 s and 60 °C for 60 s. Gene expression was normalized using U6 snRNA as an internal control. The primers (Supplemental Table 1) were designed using the Primer Premier 5.0 software (Premier Biosoft International, Silicon Valley, CA, USA). The relative quantification method (2-ΔΔCt) was used to evaluate quantitative variation between different treatments.

### 2.10. Functional annotation

Protein and gene functions were categorized using MapMan bin codes (http://mapman.gabipd.org/) [34]. The predication of identified proteins and genes derived from L. *japonica* was performed by transferring annotations to the *Arabidopsis* genome and consideration of orthologous genes. Pathway mapping of identified proteins and genes was performed using the Kyoto Encyclopedia of Genes and Genomes (KEGG) database (http://www.genome.jp/kegg/) [35].

### 2.11. Cluster analysis of differentially abundant proteins that were commonly identified during the flowering period

A hierarchical clustering analysis was generated to show the fold change ratios of the proteins. The fold change ratio was calculated as the fold change of proteins in TGS, TWS, SFS, and GFS as compared with that in JBS. The cluster analysis was performed using the pheatmap package in R [36].

### 2.12. Statistical analysis

The SPSS statistical software (version 22.0; IBM, Armonk, NY, USA) was used for statistical evaluation. Statistical significance was evaluated by the Student's *t*-test when only two groups were compared or one-way ANOVA followed by Tukey's test when multiple groups were compared. A *p*-value < .05 was considered as the statistical significance.

Data sets containing three independent biological replicates per samples were statistically analyzed. In order to assess the abundance changes between the samples and identify the proteomic changes involved in group discrimination, the principal component analysis (PCA) was performed by using the R prcomp function.

## 3. Results

### 3.1. Genes, proteins and metabolites identified during the flowering period of L. japonica

In order to determine the molecular phenotype of L. *japonica* during the flowering period, transcriptomic, proteomic, and metabolomic analyses were performed. A total of 2715, 2700, 2536, 2441, and 2483 genes were identified in JBS, TGS, CWS, SFS, and GFS, respectively. The enriched genes were mainly related to functional categories of protein metabolism, transport, signaling, and RNA metabolism (Fig. 1, Supplemental Table 2). During TGS, the number of genes related to protein metabolism, transport, cell wall, lipid metabolism, hormone metabolism, and DNA metabolism were increased compared with other developmental stages. The number of genes related to cell and secondary metabolism was gradually decreased with the progressing floral developmental stages.

A total of 291, 280, 279, 256, and 224 proteins were identified in JBS, TGS, CWS, SFS, and GFS, respectively. Identified proteins were mainly enriched to functions of protein metabolism, photosynthesis, glycolysis, and TCA cycle (Fig. 1, Supplemental Table 3). The number of proteins related to photosynthesis and transport was gradually decreased and increased, respectively, during the progressive floral developmental stages.

A total of 285, 283, 265, 248, and 251 metabolites were identified in JBS, TGS, CWS, SFS, and GFS, respectively. The identified metabolites were mainly enriched to the categories of organic acids, amino acids, carbohydrates, and alcohols (Fig. 1, Supplemental Table 4). Meanwhile, organic acids were significantly enriched in TGS. Fatty acids, esters, terpenoids, and alkaloids related metabolites were mainly enriched in JBS. The metabolites particularly related to fatty acids gradually decreased during the five floral development stages.

### 3.2. Pathway integration of identified genes, proteins, and metabolites related to cell wall, glycolysis, photosynthesis, and secondary metabolism

Based on molecular functional categorization, the numbers of genes or proteins related to photosynthesis, glycolysis, cell wall, and secondary metabolism were significantly changed during the 5 floral developmental stages. For a better understanding of the physiological adjustment of flower development of L. *japonica*, the interactive biochemical networks were constructed through the pathway integration on KEGG database (Supplemental Figs. 1A-E). The network was manually divided into 3 parts *i.e.* sugar metabolism, lipopolysaccharide biosynthesis, and carbon conversion. The numbers of genes and proteins were significantly decreased in parts of sugar metabolism and lipopolysaccharide biosynthesis. However, in carbon conversion part, the number of transcripts and proteins of pyruvate kinase (PK) was increased and decreased, respectively, with the development stages.

Identified genes, proteins, and metabolites were linked to biosynthetic pathways of terpenoids, fatty acids, vitamin E, alkaloids, lignins, and phenylpropanoids (Supplemental Figs. 2A-E). The numbers of genes involved in both phenylpropanoids and alkaloids biosynthesis pathways were significantly decreased during the floral development stages. However, genes of 1-deoxy-D-xylulose 5-phosphate reductoisomerase (DXPPRI), solanesyl-diphosphate synthase (SDPPS), and phytoene synthase (PTST) were significantly increased after JBS. The genes of lycopene beta cyclase (LBCA), beta-amyrin synthase

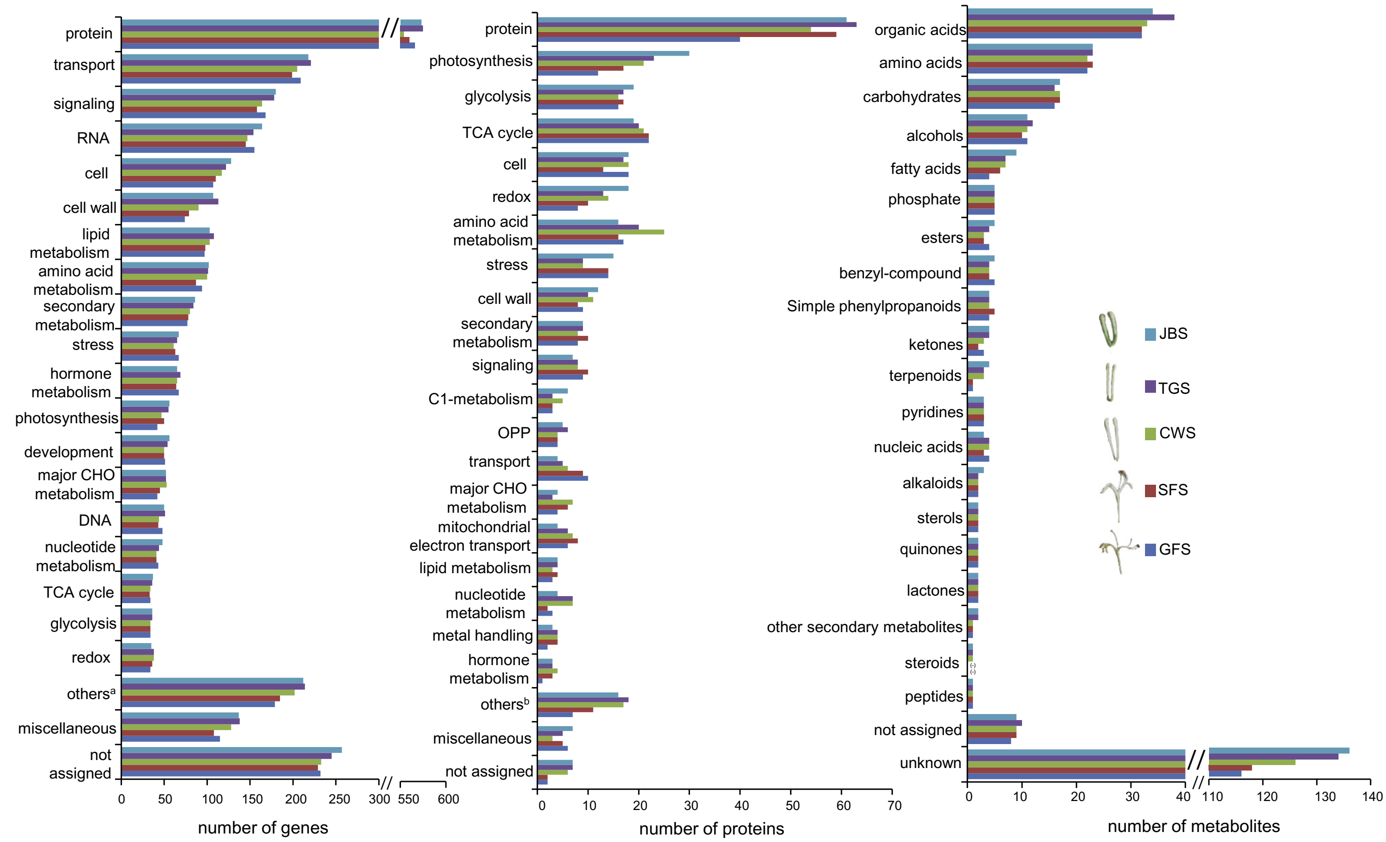


**Fig. 1.** Distribution of identified genes, proteins, and metabolites in L. *japonica* during JBS, TGS, CWS, SFS, and GFS. Genes, proteins, and metabolites were extracted from flowers of L. *japonica* in JBS, TGS, CWS, and GFS. Functions of genes and proteins were predicated and categorized using MapMan bin codes.

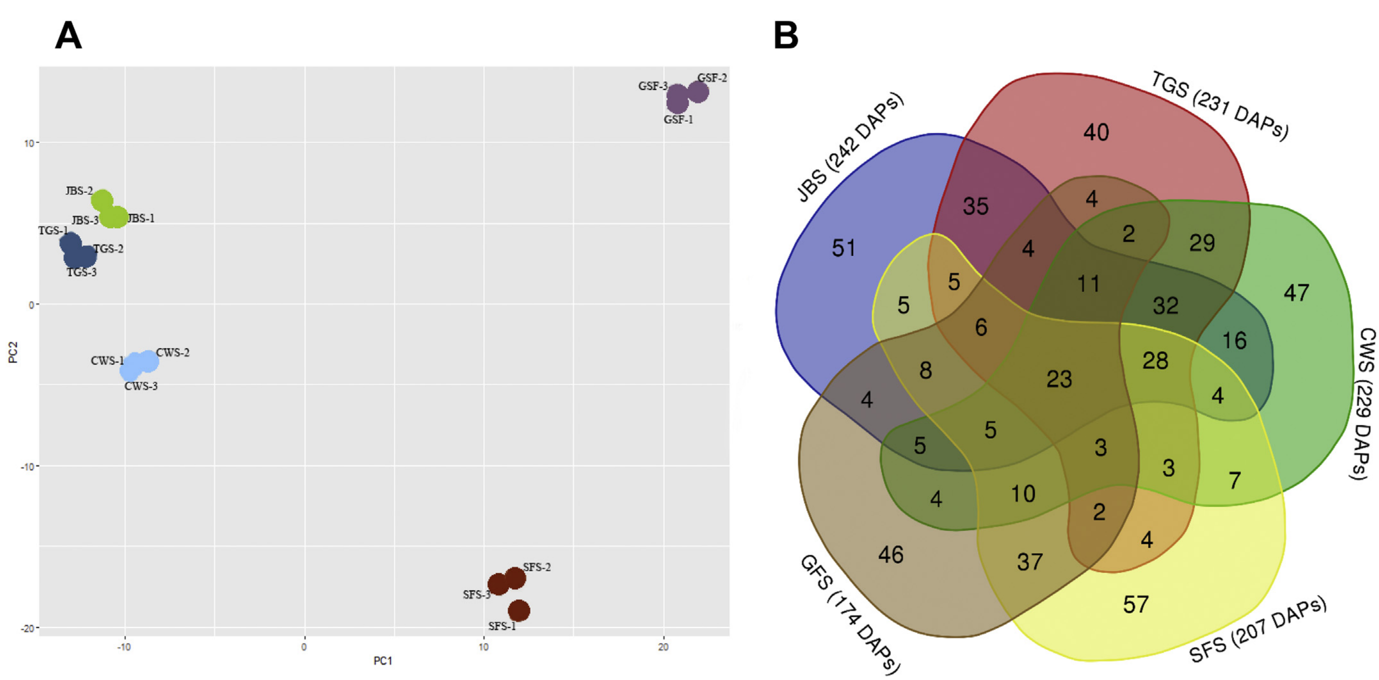


**Fig. 2.** Summary of identified proteins in L. *japonica* during JBS, TGS, CWS, SFS, and GFS. A, The PCA analysis of the identified proteins for samples JBS, TGS, CWS, SFS, and GFS; B, Venn diagram showing the overlap of differentially expressed proteins from differential floral stages.

(BAST), 3-hydroxy-3-methylglutaryl-coenzyme A reductase (HMCR) were upregulated in SFS and GFS compared with JBS and TGS. The identified secondary metabolism related proteins were mainly involved in phenylpropanoids and terpenoids biosynthesis pathways. Interestingly, a total of 5 proteins were identified in the terpenoid biosynthetic pathways which were not expressed in JBS. In phenylpropanoids biosynthetic pathways, 8-Hydroxygeraniol dehydrogenase (HDGD), beta-glucosidase (BGD), and chalcone synthase (CHS) was

**Table 1**
List of 23 common DAPs during the five developmental stages of L. *japonica* flower.

| | | | | Mol% | | | | | | |
|---|---|---|---|---|---|---|---|---|---|---|
| no | ID | Description | Mass | JBS | TGS | CWS | SFS | GFS | p_value | Function |
| 1 | Q42962 | Phosphoglycerate kinase, cytosolic | 42,338 | 0.26 | 0.29 | 0.37 | 0.46 | 0.57 | 0.02366 | Glycolysis |
| 2 | P11143 | Heat shock 70 kDa protein | 70,871 | 0.33 | 0.32 | 0.34 | 0.36 | 0.54 | 0.00064 | Stress |
| 3 | P54774 | Cell division cycle protein 48 homolog | 90,512 | 0.32 | 0.25 | 0.22 | 0.29 | 0.45 | 0.00129 | Cell |
| 4 | Q9SCN8 | Cell division control protein 48 homolog D | 91,082 | 0.33 | 0.26 | 0.25 | 0.32 | 0.41 | 0.01114 | Cell |
| 5 | P08927 | RuBisCO large subunit-binding protein subunit beta, chloroplastic | 63,287 | 0.20 | 0.23 | 0.24 | 0.24 | 0.38 | 0.00674 | Protein |
| 6 | Q2R1V8 | GDP-mannose 3,5-epimerase 2 | 42,504 | 0.19 | 0.14 | 0.14 | 0.19 | 0.36 | 0.00412 | Redox |
| 7 | P49612 | S-adenosylmethionine synthase 1 | 40,314 | 0.26 | 0.19 | 0.22 | 0.21 | 0.35 | 0.00681 | Amino acid meta. |
| 8 | Q9ZSQ4 | Phosphoglucomutase, cytoplasmic | 63,369 | 0.14 | 0.12 | 0.14 | 0.27 | 0.33 | 0.00000 | Glycolysis |
| 9 | Q9FGX1 | ATP-citrate synthase beta chain protein 2 | 66,356 | 0.12 | 0.11 | 0.12 | 0.21 | 0.28 | 0.00573 | TCA cycle |
| 10 | F4K0E8 | 4-hydroxy-3-methylbut-2-en-1-yl diphosphate synthase (ferredoxin), chloroplastic | 82,832 | 0.12 | 0.10 | 0.07 | 0.27 | 0.28 | 0.00006 | Secondary meta. |
| 11 | P08735 | Glyceraldehyde-3-phosphate dehydrogenase 1, cytosolic | 36,614 | 0.17 | 0.17 | 0.17 | 0.23 | 0.27 | 0.01666 | Glycolysis |
| 12 | Q05046 | Chaperonin CPN60–2, mitochondrial | 61,434 | 0.16 | 0.16 | 0.16 | 0.10 | 0.25 | 0.01690 | Protein |
| 13 | P20422 | Plastocyanin | 10,232 | 0.16 | 0.16 | 0.16 | 0.19 | 0.25 | 0.00000 | Photosynthesis |
| 14 | P34794 | RuBisCO large subunit-binding protein subunit alpha, chloroplastic | 61,682 | 0.13 | 0.10 | 0.19 | 0.17 | 0.25 | 0.00006 | Photosynthesis |
| 15 | O49845 | Sucrose synthase isoform 2 | 92,106 | 0.13 | 0.09 | 0.09 | 0.14 | 0.23 | 0.00046 | Major CHO meta. |
| 16 | O23755 | Elongation factor 2 | 94,708 | 0.15 | 0.19 | 0.14 | 0.16 | 0.22 | 0.01485 | Protein |
| **17** | **O20250** | **Transketolase, chloroplastic** | **80,744** | **0.05** | **0.09** | **0.05** | **0.12** | **0.15** | **0.00154** | **Photosynthesis** |
| 18 | Q38799 | Pyruvate dehydrogenase E1 component subunit beta-1, mitochondrial | 39,436 | 0.05 | 0.06 | 0.06 | 0.07 | 0.13 | 0.00741 | TCA cycle |
| 19 | P29356 | Fructose-bisphosphate aldolase, cytoplasmic isozyme | 38,675 | 0.04 | 0.04 | 0.04 | 0.04 | 0.06 | 0.00002 | Glycolysis |
| 20 | Q9FIK7 | Probable acetyl-CoA acetyltransferase, cytosolic 2 | 43,664 | 0.03 | 0.03 | 0.03 | 0.04 | 0.05 | 0.00000 | Amino Acid meta. |
| 21 | Q94A28 | Aconitate hydratase 3, mitochondrial | 1E + 05 | 0.03 | 0.03 | 0.03 | 0.04 | 0.05 | 0.01813 | TCA cycle |
| 22 | Q38798 | Calnexin homolog 2 | 60,737 | 0.02 | 0.02 | 0.02 | 0.03 | 0.04 | 0.00001 | Signaling |
| **23** | **P37142** | **Bifunctional aspartokinase/homoserine dehydrogenase, chloroplastic** | **1E + 05** | **0.04** | **0.05** | **0.04** | **0.03** | **0.02** | **0.00009** | **Amino acid meta.** |

Footnote: meta., metabolism; TCA, tricarboxylic acid; CHO, carbohydrate.
The first proteins in cluster I and II in Fig 3, respectively, were shown in bold in Table 1.

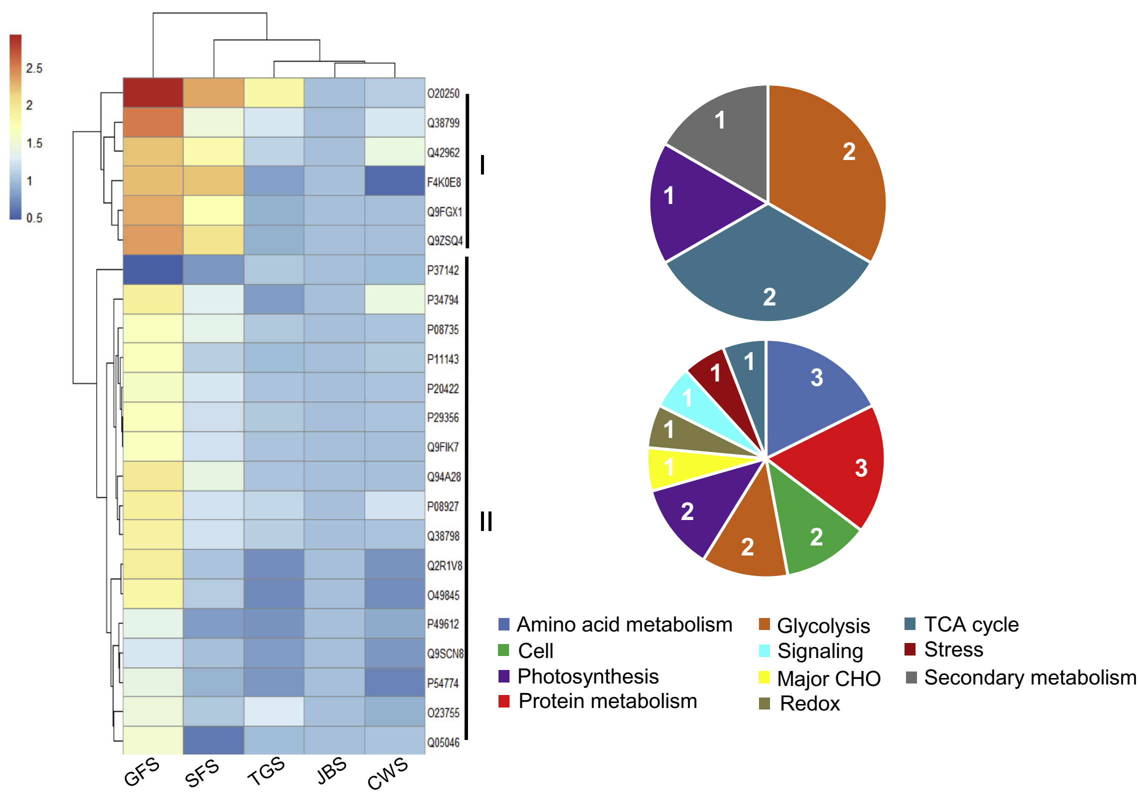


**Fig. 3.** Cluster and functional categorization analyses of changed proteins in L. *japonica* during the flower development. Proteins were extracted from the flowers of L. *japonica* in JBS, TGS, CWS, SFS, and GFS. A total of 23 common DAPs were examined by cluster analysis based on their abundance ratios and were clustered in to 2 groups. Proteins were functionally categorized using MapMan bin codes. A total of 11 functional categories were recognized for Clusters I and II. The numbers in the pie graphs correspond to the protein number. Abbreviations: CHO, carbohydrate; TCA, tricarboxylic acid.

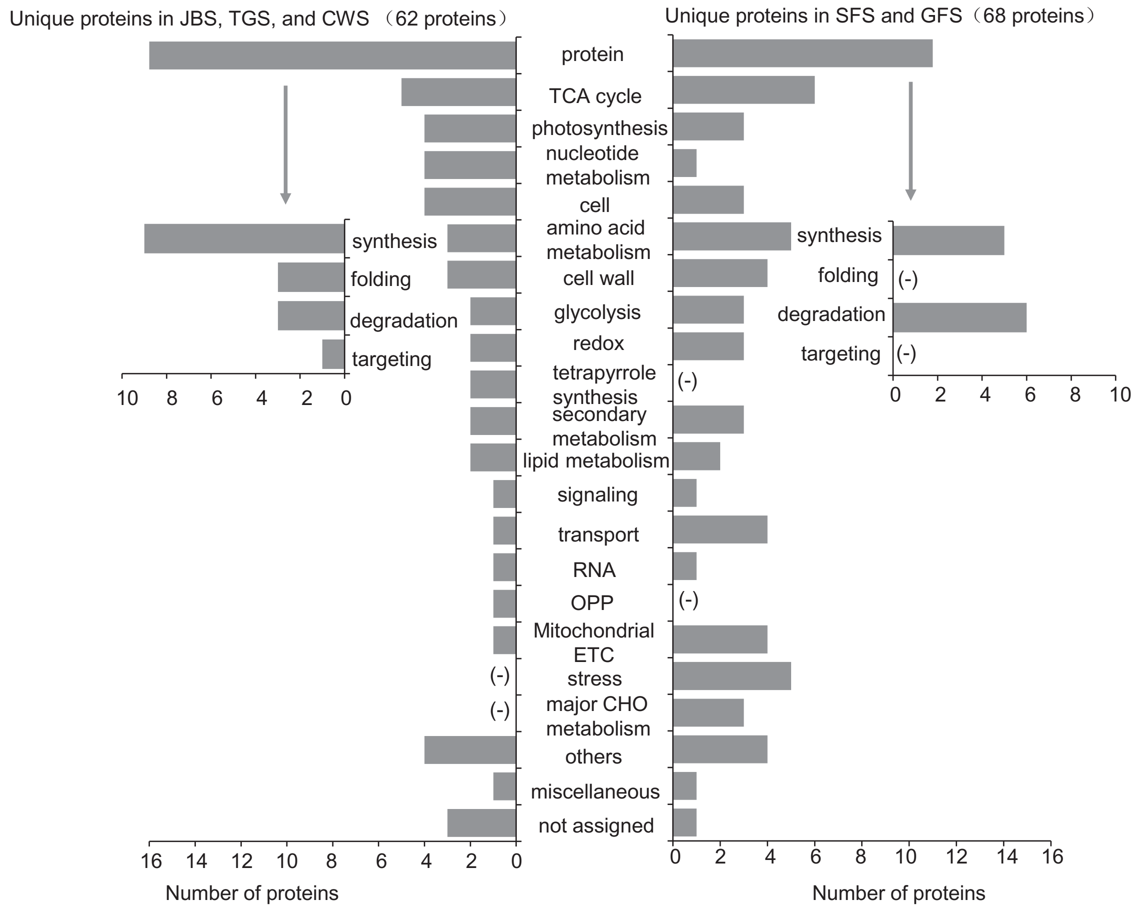


**Fig. 4.** Functional distribution of proteins which were respectively unique in early and late stages of flower development. Protein functions were predicted and categorized using MapMan bin codes. "( − )" indicates that there's no proteins were categorized. Abbreviations: TCA, tricarboxylic acid; OPP, oxidative pentose phosphate; ETC, electron transport chain; CHO, carbohydrate.

expressed in TGS, CWS, and JBS, respectively. The number of transcripts of 4-coumarate–CoA ligase (4CL) was decreased in GFS as compared with the earlier 4 stages.

### *3.3. The comprehensive proteomic analysis of the flowers of L. japonica during the developmental stages*

To get a comprehensive understanding of floral development at proteomic level, the expression profiles of all the identified proteins during the floral developmental stages were analyzed by PCA (Fig. 2A). Both the first and second principal components (PC1 (34.6%) and PC2 (19.7%)) explained the variance across the dataset. Furthermore, the late period (SFS and GSF) was well separated from the early period (JBS, TGS, and CWS) in PC1. In order to deeply reveal the potential variance in the floral period, the change of identified proteins among 5 developmental stages was evaluated by a multivariate statistical analysis using ANOVA approach. A total of 538 differentially abundant proteins (DAPs) were selected and employed for the further analysis (Supplemental Table 5). The Venn diagram was generated to show the overlap of the DAPs from 5 stages (Fig. 2B). There were 242, 231, 229, 207, and 174 DAPs in JBS, TGS, CWS, SFS, and GFS, respectively. Among these DAPs, abundances of 51, 40, 47, 57 and 46 proteins were specifically changed during the JBS, TGS, CWS, SFS, and GFS, respectively.

### *3.4. Cluster and functional analyses of commonly identified DAPs in L. japonica flower during the developmental stages*

In order to understand the abundance profile of the commonly identified DAPs (cDAPs) in *L. japonica* flower during the five developmental stages, the hierarchical clustering analysis was performed. The abundances of 23 proteins were commonly changed during the five developmental stages of L. *japonica* flower (Fig. 2, Table 1). The cDAPs in TGS, CWS, SFS, and GFS were compared with SFS. The 23 cDAPs were analyzed by cluster analysis based on their abundance ratios. Using a hierarchical clustering analysis, two clusters (I and II) of the cDAPs were formed (Fig. 3). Cluster I consisted of 6 proteins that increased abundance during SFS and GFS while decreased during JBS, TGS, and CWS. Cluster II contained 17 proteins, 16 proteins of which were increased in GFS while decreased during JBS, TGS, CWS, and SFS. Furthermore, transketolase (TK) in cluster I and bifunctional aspartokinase/homoserine dehydrogenase in cluster II were 2-fold increase and 1-fold decrease in GFS, respectively, compared with JBS (Fig. 3).

The functions of these common proteins changed during developmental stages of L. *japonica* flower were predicted with functional annotations of the *Arabidopsis* genome and classified using MapMan bin codes (Fig. 3). A total of 11 functional categories were recognized for Clusters I and II. The cDAPs present in Cluster I were related to glycolysis, TCA cycle, photosynthesis, and secondary metabolism. The cDAPs present in Cluster II were mainly related to amino acid metabolism, protein metabolism, cell, glycolysis, and photosynthesis.

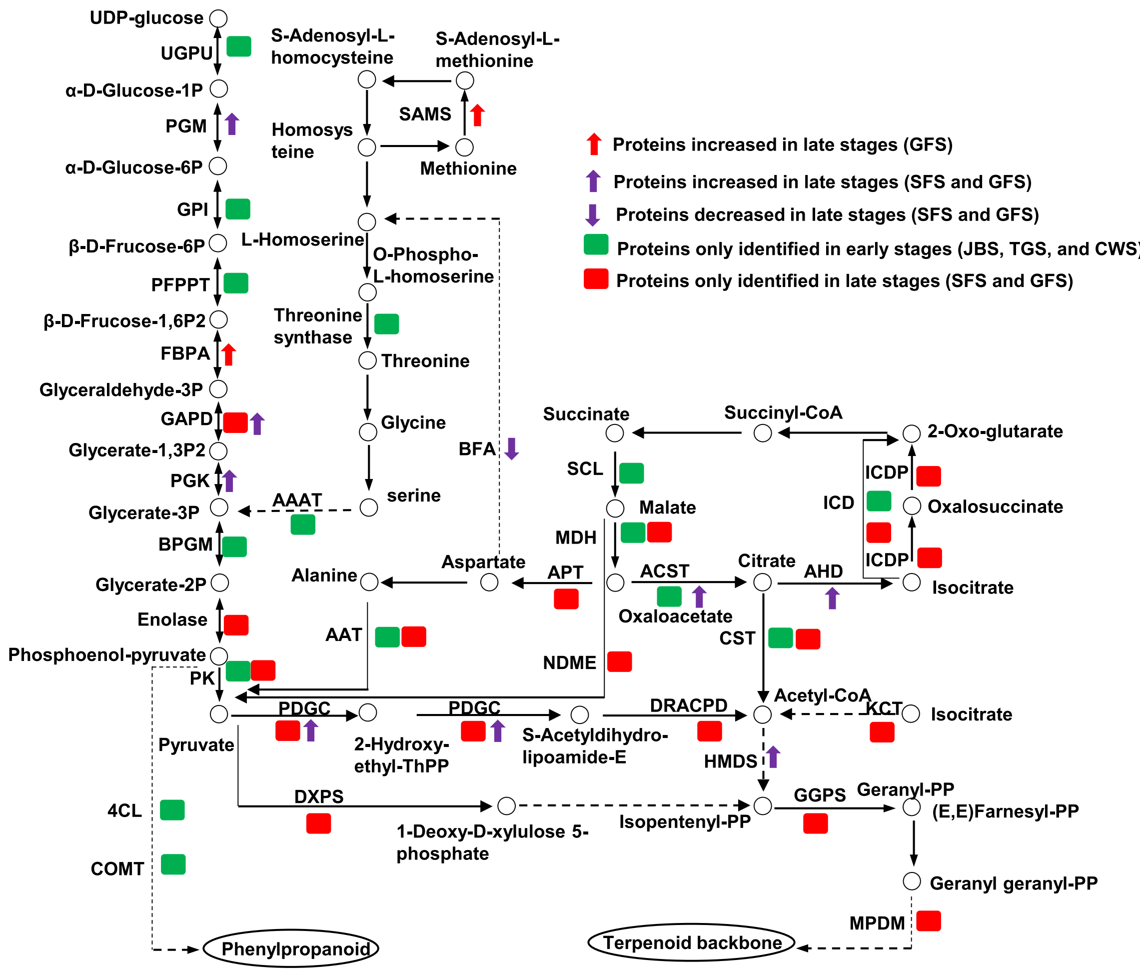


**Fig. 5.** Integrated pathways of proteins involved in glycolysis, TCA cycle, amino acid metabolism, and secondary metabolism in Fig. 4. Pathways were mapped using the KEGG database. Abbreviations: AAAT, branched-chain-amino-acid aminotransferase 5; ACST, ATP-citrate synthase beta chain protein 1; BPGM, 2,3-bisphosphoglycerate-independent phosphoglycerate mutase; 4CL, 4-coumarate–CoA ligase; COMT, caffeic acid 3-*O*-methyltransferase; CST, citrate synthase; DXPS, 1-deoxy-D-xylulose-5-phosphate; DRACPD, dihydrolipoyllysine-residue acetyltransferase component 2 of pyruvate dehydrogenase complex; GAPD, glyceraldehyde-3-phosphate dehydrogenase; GGPS, geranylgeranyl pyrophosphate synthase; GPI, glucose-6-phosphate isomerase; UGPU, UTP–glucose-1-phosphate uridylyltransferase; ICD, isocitrate dehydrogenase [NAD] catalytic subunit 5; ICDP, Isocitrate dehydrogenase [NADP]; KCT, 3-ketoacyl-CoA thiolase 1; MDH, malate dehydrogenase; MPDM, 2-methyl-6-phytyl-1,4-hydroquinone methyltransferase; NDME, NAD-dependent malic enzyme 2; PDGC, pyruvate dehydrogenase E1 component subunit alpha; PFPPT, pyrophosphate–fructose 6-phosphate 1-phosphotransferase subunit beta; PGM, phosphoglucomutase; PK, pyruvate kinase; SCL, succinyl-CoA ligase [ADP-forming] subunit beta; HMDS, 4-hydroxy-3-methylbut-2-en-1-yl diphosphate synthase; SAMS, S-adenosylmethionine synthase; AAT, alanine aminotransferase; APT, aspartate aminotransferase; FBPA, fructose-bisphosphate aldolase; AHD, aconitate hydratase.

### *3.5. Functional analysis of uniquely identified proteins during early and late developmental stages of L. japonica flower*

In order to determine the molecular mechanisms for secondary metabolism during the developmental stages of L. *japonica*, the unique proteins identified during early and late stages were analyzed. A total of 62 and 68 proteins were unique in early and late stages, respectively (Fig. 4). Based on the functional analysis, the unique proteins in early stages were mainly related to protein metabolism, TCA cycle, photosynthesis, nucleotide metabolism, cell, amino acid metabolism, cell wall, and glycolysis. On the other hand, unique proteins in late stages were mainly related to protein metabolism, TCA cycle, amino acid metabolism, cell wall, transport, and mitochondrial electron transport chain (ETC). The number of unique DAPs related to transport was significantly increased in late stages compared with early stages. However, the number of unique DAPs related to nucleotide metabolism was significantly decreased in late stages compared with early stages. Furthermore, unique DAPs related to protein folding, protein targeting, tetrapyrrole synthesis, and oxidative pentose phosphate were not identified in late stages while DAPs related to stress and major CHO metabolism were not identified in early stages (Fig. 4).

### *3.6. Pathway integration of unique DAPs in early and late stages of L. japonica*

In order to obtain a deeper insight into secondary metabolism of L. *japonica*, the DAPs related to glycolysis, TCA cycle, amino acid metabolism, and secondary metabolism were mapped into pathways using KEGG pathway (Fig. 5). UTP–glucose-1-phosphate uridylyltransferase (UGPU), glucose-6-phosphate isomerase (GPI), pyrophosphate–fructose 6-phosphate 1-phosphotransferase subunit beta (PFPPT), 2,3-bisphosphoglycerate-independent phosphoglycerate mutase (BPGM), threonine synthase, and branched-chain-amino-acid aminotransferase (AAAT) which were involved in phosphoenol-pyruvate formation were only identified in early stages. Glyceraldehyde-3-phosphate dehydrogenase 2 and enolase were unique in late stages. The common DAPs glyceraldehyde-3-phosphate dehydrogenase 1 and phosphoglycerate kinase (PGK) were increased in SFS and GFS while fructose-bisphosphate aldolase (FBPA) was increased in GFS compared with early stages. In amino acid metabolism, proteins mainly in pathway fluxing

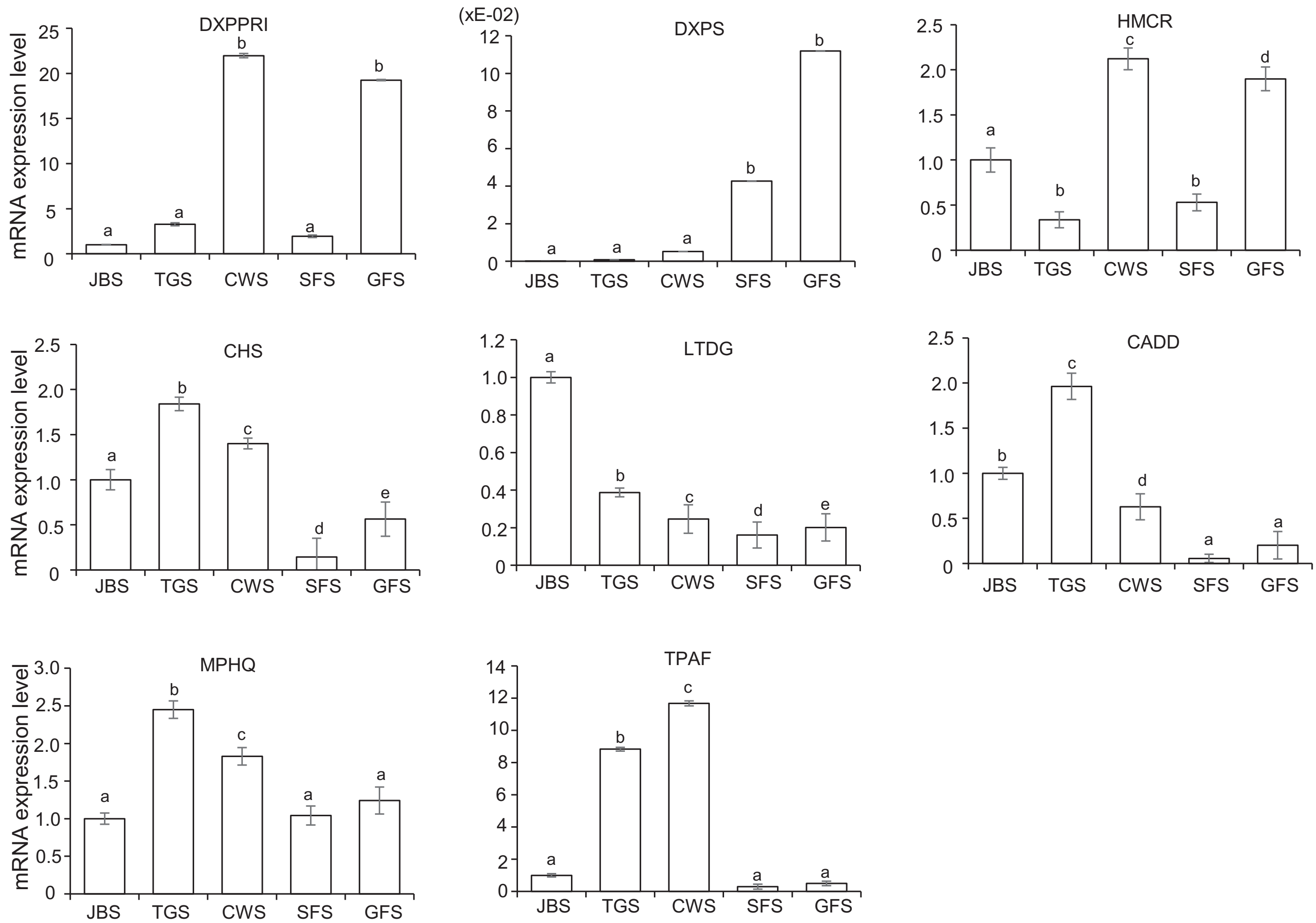


**Fig. 6.** Expression level of selected genes in L. *japonica* from developmental stages. Flowers of L. *japonica* were collected at JBS, TGS, CWS, SFS, and GFS. RNAs were extracted and the expression of genes was measured by qRT-PCR. The data are presented as the mean ± S.D. from 3 independent biological replicates. Means with the same letter were not significantly different among floral stages while different letters indicate that the change is significant according to Tukey's multiple comparison ($p < .05$).

to glycerate-2P were unique in early stages; however, proteins in pathway fluxing to pyruvate and acetyl-CoA were unique in late stages. In TCA cycle pathways, succinyl-CoA ligase [ADP-forming] subunit beta (SCL), isocitrate dehydrogenase [NAD] regulatory subunit 1, malate dehydrogenase (MDH), ATP-citrate synthase beta chain protein, and citrate synthase (CST) were unique in early stages. Isocitrate dehydrogenase [NAD] catalytic subunit 5 (ICD), NAD-dependent malic enzyme 2 (NDME), isocitrate dehydrogenase [NADP] (ICDP), MDH, pyruvate dehydrogenase E1 component subunit alpha (PDGC), and dihydrolipoyllysine-residue acetyltransferase component 2 of pyruvate dehydrogenase complex (DRACPD) were unique in late stages. Furthermore, ACST and aconitate hydratase (AHD) were increased in SFS and GFS. In secondary metabolism, 4CL and caffeic acid 3-*O*-methyltransferase (COMT), involved in phenylpropanoid pathways, were unique in early stages. Geranylgeranyl pyrophosphate synthase (GGPS), 1-deoxy-D-xylulose-5-phosphate (DXPS), and 2-methyl-6-phytyl-1,4-hydroquinone methyltransferase (MPDM), involved in terpenoid backbone pathways, were unique in late stages. Furthermore, PDGC and 4-hydroxy-3-methylbut-2-en-1-yl diphosphate synthase (HMDS) were increased in SFS and GFS compared with early stages (Fig. 5).

### *3.7. qRT-PCR analysis of secondary metabolism related genes*

The expression of genes related to terpenoids, alkaloids, fatty acids, and phenylpropanoids was altered during the developmental stages of L. *japonica* (Supplemental Fig. 2). These differentially expressed genes from these groups were selected for the mRNA expression analysis. The mRNA expression levels of DXPS, DXPPRI, HMCR, TPAF, MPHQ, CHS, 4CL, CADD, and LTDG were analyzed by qRT-PCR (Fig. 6). DXPPRI and HMCR genes related to terpenoids pathway were highly upregulated in CWS and GFS. Whereas, DXPS gene related to terpenoids pathway were highly upregulated during SFS and GFS. On the other hand, in phenylpropanoids pathway, CHS and CADD genes were upregulated in JBS, TGS, and CWS, whereas LTDG genes were upregulated in JBS. MPHQ and TPAF genes related to vitamin E and alkaloids pathways, respectively, were upregulated during TGS and CWS.

### *3.8. Analysis of secondary metabolites accumulation during the flower development stages of L. japonica*

In order to find out the changes in secondary metabolism during the developmental stages of *L. japonica*, the differential accumulation of secondary metabolites related to simple phenylpropanoids and flavonoids were analyzed (Figs. 7 and 8). The intensity of phenylalanine was approximately four times higher in TGS as compared with other stages. The 4-coumarate accumulated significantly in TGS and CWS while the intensity of chlorogenic acid was higher in JBS, TGS, and CWS as compared with SFS and GFS (Fig. 7). The intensity of apigenin and neohesperidin related to phenylpropanoids in JBS was higher than the following 4 stages. Luteolin accumulated during the early stages (JBS,

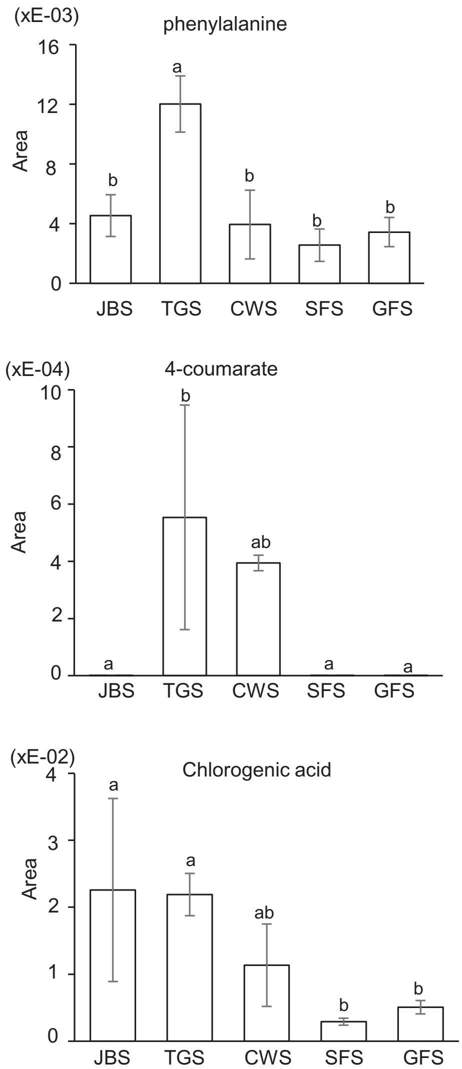


**Fig. 7.** Accumulation of phenylpropanoids in L. *japonica.* Identified phenylpropanoids were extracted from metabolomic database obtained by GC TOF/MS. The mothed of interquartile range denoising was used for quantification of metabolites and total area of each sample integration area was normalized for each sample. The data are presented as the mean ± S.D. from 6 independent biological replicates. Means with the same letter were not significantly different among floral stages while different letters indicate that the change is significant according to Tukey's multiple comparison ($p < .05$).

TGS, and CWS) and then decreased in the later developmental stages (SFS and GFS). Quercetin and quercetin 3-o-glucoside were identified only in JBS (Fig. 8).

## 4. Discussion

### 4.1. Metabolic changes during the flower developmental stages of L. japonica

In the present study, transcriptomic, proteomic, and metabolomic analysis of L. *japonica* flower were conducted for an integrated view of the dynamic changes during the developmental period. $CO_2$ fixation in the petals of flower buds is required during the early stages of flower development [37]. The photosynthesis related genes were down-regulated with the progressing flower development in *Arabidopsis* and snapdragon [38–39]. Furthermore, cell growth, cell wall synthesis, small molecule biosynthesis, and photosynthesis related genes were down-regulated during flower development in snapdragon [38]. In this study, the numbers of genes related to cell and secondary metabolism and proteins related to photosynthesis gradually decreased during the flower development (Fig. 1), indicating important biochemical switches occurred during the flower development of L. *japonica*.

Actually, loose correlation between mRNA and protein levels existed during the floral stages of L. *japonica* (Fig. 1, Supplemental Fig. 1). Until recently, studies have shown that the correlation between mRNA and protein expressions can be low due to various factors such as post transcription regulation. The stimulus, immune system process, and reproduction showed significant differences between transcript abundance and protein abundance in white spruce stems during the transition from active growth to dormancy [40]. The inconsistent expression patterns at mRNA and protein levels also occurred during rice early post-pollination [41]. Protein abundances reflect a dynamic balance among linked processes, spanning the transcription, processing, and degradation of mRNA to the translation, localization, modification, and programmed destruction of the proteins themselves. In order to reveal the potential molecular mechanisms underlying the floral development, the identified proteins were further analyzed in this study. However, it is undeniable that the current results leave the directions on exploring the roles for the many regulatory mechanisms occurring after mRNAs during the floral development.

### 4.2. Fatty acids affect early flower bud induction

Changes in fatty acid (FA) composition has a number of effects on plant development. Unsaturated FAs are the sources of reactive oxygen species production [42]. The triple mutant of *fatty acid desaturase 3* (*fad3*), *fad7*, and *fad8* in *Arabidopsis* produced negligible linolenic acid, leading to a low level of jasmonic acid (JA) content [43]. Pollen development is critical for linolenic acid or JA as severe reduction of the linolenic acid (LA) in *Arabidopsis* resulted in male sterility [43]. LA is one of the precursors for JA biosynthesis [44] and the lipoxygenase (a key enzyme for JA biosynthesis) [45], and it affects flower bud induction [46]. Furthermore, the LA cascade products like 9,10-α-ketol-octadecadienoic acid have strong flower-inducing activity [47]. In this study, it was demonstrated that unsaturated FAs had higher content in the early stages in L. *japonica* than the later stages (Supplemental Table 4). The high expression of lipoxygenase (Supplemental Table 2) and accumulation of LA (Supplemental Table 4) might perform an important role in inducing the early flower bud by increasing the JA level and accumulating LA cascade products.

### 4.3. Phenylpropanoids pathway was activated in the early stages of flower development

Glycolysis is essential for energy provision in heterotrophic cells as well as for wide range of other physiological functions. The intermediates of glycolysis serve as precursor for primary and secondary metabolites [48]. The identification of unique proteins involved in glycolysis in the early stages indicated that glycolysis might be in active state in early stages (Fig. 5). As it was proved that the activated glycolysis contributed to the accumulation of phenylpropanoids through the shikimic acid pathway [49–50]. Previous study demonstrated that the content of chlorogenic acid was higher in bud stage than that in flower stage [7]. As the active compounds of L. *japonica*, chlorogenic acid, luteolin, and their precursors (phenylalanine and 4-coumarate) were observed to reduce in late stage (Figs. 7 and 8). Flavonoids play a key role in cellular protection under biotic and abiotic stresses [51–53], elimination of reactive oxygen species [54], and constitution of flower color pigment [55]. These results indicate that the significant accumulation of phenylpropanoids in the early stages from the activated glycolysis might endow high stress tolerance to the early flower cells of L. *japonica* and give us theoretical support for the utilization of L. *japonica* as medicinal materials.

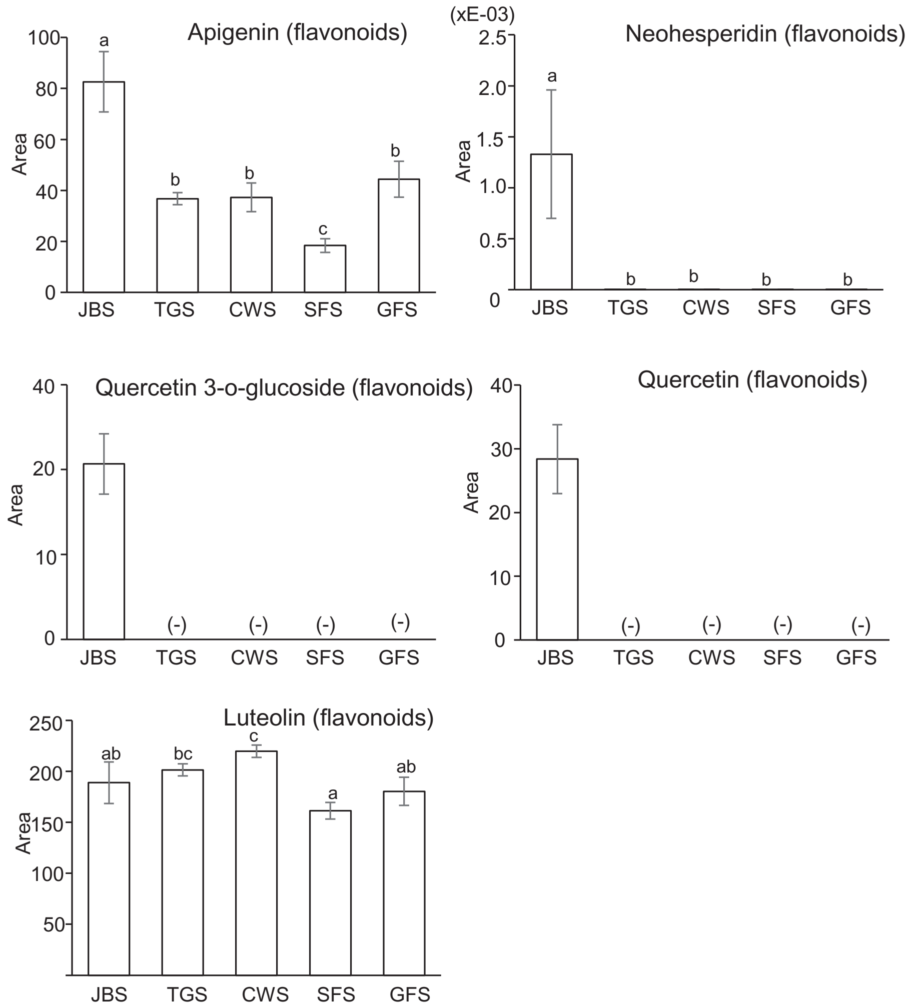


**Fig. 8.** Accumulation of flavonoids, terpenoids, and alkaloids in L. *japonica*. UPLC TOF MS/MS and GC TOF/MS were used for metabolites identification. Secondary metabolites were extracted from metabolomic database obtained by GC TOF/MS or analyzed by LC TOF MS/MS. For GC TOF/MS, the mothed of interquartile range denoising was used for quantification of metabolites and total area of each sample integration area was normalized for each sample. For UPLC TOF MS/MS, total sum area module was used for total ion chromatogram normalization and the normalized intensities were integrated for each sample. "(−)" means that the metabolite was not detected. All data are shown as the mean ± SD from 3 independent biological replicates. Means with the same letter were not significantly different among floral stages while different letters indicate that the change is significant according to Tukey's multiple comparison ($p < .05$).

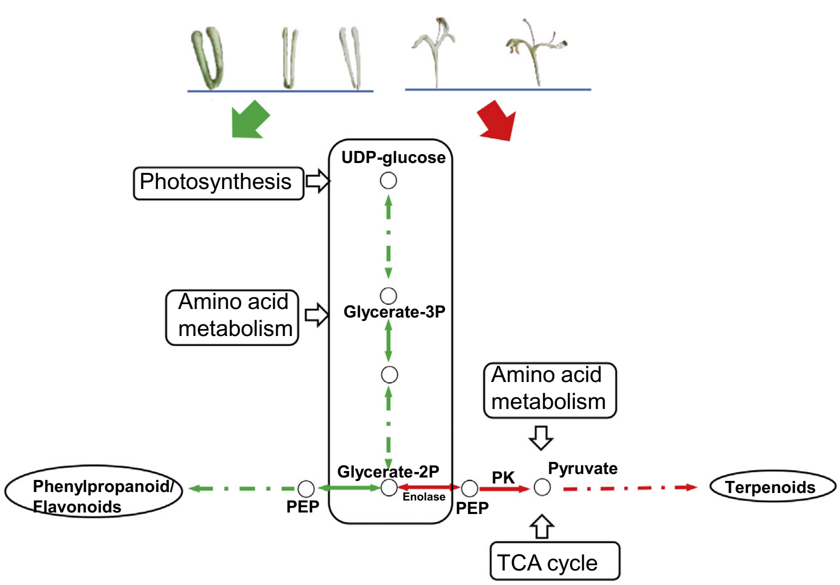


**Fig. 9.** The summary diagram of major findings in this study.

### 4.4. *Transketolase might regulate the activity of terpenoids backbone pathway in the late stages*

TK functions in the Calvin Benson (C3) cycle that has significant effect on plant photosynthesis and growth. C3 cycle fixing carbon into sucrose and starch is essential for the biosynthesis of aromatic amino acids and phenylpropanoids [56] and for isoprenoid biosynthesis from the methylerythritol pathway (MEP). A study demonstrated a small reduction in the TK activity inhibited photosynthesis and significantly decreased the levels of aromatic amino acids and phenylpropanoids [57]. Our study showed a downward trend on the whole of the process from erythrose 4-phosphate to ribulose 1,5-bisphosphate based on the number of genes and proteins during the floral development of L. *japonica* (Supplemental Fig. 1). As this process is not only essential for maintaining active photosynthesis, but also provide the precursor metabolites for phenylpropanoid metabolism [58], it was inferred that the increased TK might play little role on promoting the photosynthesis and phenylpropanoid metabolism. As a confirmation, we proved that the number of photosynthesis related genes and proteins was decreased (Fig. 1) and metabolites in phenylpropanoid metabolism were reduced or no increased at least in the late stages than those in the early stages (Figs. 7 and 8).

It was proved that TK also plays role on MEP pathway [59]. As a product of TK, glyceraldehyde 3-phosphate (G3P) can be transferred into DXPS by the action of deoxylulose-5-phosphate synthase (DXS) in MEP pathway. TK activity needs the presence of thiamine pyrophosphate (TPP) which is synthesized from thiamine, while the formation of thiamine is dependent on the G3P. This regulatory circuit was proved to exist to coordinate TK activity with availability of TPP [60]. The roles of TK in pepper fruits during the early onset of isoprenoid biogenesis was illustrated that overexpressed TK furnished the isopentenyl diphosphate necessary for increased carotenoid biosynthesis [61]. In our current study, FBPA, glyceraldehyde-3-phosphate dehydrogenase 2 (GAPD2), and PGK were increased in GFS compared with early stages and GAPD1 was unique in late stages, indicating an increased accumulation of G3P. TK was significantly increased in late stages compared with early stages and the MEP pathway related proteins DXPS, GGPS, and MPDM were unique in the late stages (Fig. 5). It has been demonstrated that the content of secologanic acid was increased during flower opening in L. *japonica* [7]. These results indicate that TK-contained regulatory circuit might be activated to contribute to the biosynthesis of terpenoid backbone in the late floral stages of L. *japonica*.

DXPS catalyzes the pyruvate to form DXP, which is used for the production of isopentenyl pyrophosphate and dimethylallyl pyrophosphate [62]. Pyruvate can also be transformed into acetyl-CoA, a key precursor for terpenoids biosynthesis in plant [63–64]. In this study, enolase, pyruvate kinase 2, NDME, aspartate aminotransferase, and alanine aminotransferase (AAT) were uniquely identified in late stages of flower development of L. *japonica* (Fig. 5), indicating the increased accumulation of pyruvate with the senescence of L. *japonica* flowers. Since it was pointed that pyruvate was also involved in the TK-contained regulatory circuit [58], it was facilitated as the key substance for the metabolic flux conversion in the flower of L. *japonica* from phenylpropanoids to terpenoids biosynthesis during the floral developmental stages (Fig. 9).

## 5. Conclusion

*L. japonica* is being used for the treatment of various diseases. In order to reveal the regulatory mechanism of secondary metabolites, transcriptomic, proteomic, and metabolomic analysis was performed. The main findings are as follows: (i) the number of genes related to cell and secondary metabolism gradually decreased during the floral stages; (ii) the number of proteins related to photosynthesis and transport gradually decreased during the floral stages; (iii) the number of metabolites related to fatty acids gradually decreased during the floral stages; (iv) proteins and genes related to secondary metabolism were mainly involved in terpenoids, fatty acids, vitamin E, alkaloids, lignin, and flavonoids biosynthetic pathways; (v) DAPs were mainly involved in glycolysis/phenylpropanoid pathway and tricarboxylic acid cycle/terpenoid backbone pathway in early and late stages of flower development, respectively; (vi) phenylpropanoids pathways were activated in early stages while terpenoids pathways were promoted in late stages. The results indicate a significant metabolic flux conversion on pyruvate metabolism during the flower development of L. *japonica*, providing the explanation for the differential accumulation of flavonoids and terpenoids in the flower development stages of L. *japonica* (Fig. 9).

Supplementary data to this article can be found online at https://doi.org/10.1016/j.jprot.2019.103470.

## Acknowledgement

This work was supported by National Natural Science Foundation of China (Grant No. 81703634 and 81872973), Zhejiang Provincial Science and Technology Planning Project (Grant No. 2016C04005).

## References

[1] X. Shang, H. Pan, M. Li, X. Miao, H. Ding, *Lonicera japonica* Thunb.: ethnopharmacology, phytochemistry and pharmacology of an important traditional Chinese medicine, J. Ethnopharmacol. 138 (2011) 0–21.
[2] R. Atiqur, S.C. Kang, In vitro control of food-borne and food spoilage bacteria by essential oil and ethanol extracts of *Lonicera japonica* Thunb, Food Chem. 116 (2009) 670–675.
[3] S.L. Lee, K.H. Son, H.W. Chang, S.S. Kang, H.P. Kim, Antiinflammatory activity of *Lonicera japonica*, Phytother. Res. 12 (1998) 445–447.
[4] S. Ma, J. Du, P. But, X. Deng, Y. Zhang, Antiviral Chinese medicinal herbs against respiratory syncytial virus, J. Ethnopharmacol. 79 (2002) 205–211.
[5] Y. Yuan, L. Qi, J. Yu, X. Wang, L. Huang, Transcriptomewide analysis of SAMe superfamily to novelty phosphoethanolaminen-methyltransferase copy in *Lonicera japonica*, Int. J. Mol. Sci. 16 (2014) 521–534.
[6] L. Zhang, X. Li, W. Zheng, Z. Fu, W. Li, L. Ma, K. Li, L. Sun, J. Tian, Proteomics analysis of UV-irradiated *Lonicera japonica* Thunb. With bioactive metabolites enhancement, proteomics 13 (2013) 3508–3522.
[7] W. Zhu, W. Zheng, X. Hu, L. Zhang, J. Tian, Variations of metabolites and proteome in *Lonicera japonica* Thunb. Buds and flowers under UV radiation, BBA-Proteins Proteom. 1865 (2017) 404–413.
[8] K. Jiang, Y. Pi, R. Hou, H. Zeng, Z. Huang, Z. Zhang, X. Sun, K. Tang, Molecular cloning and expression profiling of the first specific jasmonate biosynthetic pathway gene allene oxide synthase from *Lonicera japonica*, Mol. Biol. Rep. 36 (2009) 487–493.
[9] P. Boss, R. Bastow, J. Mylne, C. Dean, Multiple pathways in the decision to flower: enabling, promoting, and resetting, Plant Cell 16 (2004) S18–S31.
[10] Y. Komeda, Genetic regulation of time to flower in *Arabidopsis thaliana*, Annu. Rev. Plant Biol. 55 (2004) 521–535.
[11] W. van Doorn, U. Van Meeteren, Flower opening and closure: a review, J. Exp. Bot. 54 (2003) 1801–1812.
[12] C. Moehs, L. Tian, K. Osteryoung, D. Dellapenna, Analysis of carotenoid biosynthetic gene expression during marigold petal development, Plant Mol. Biol. 45 (2001) 281–293.
[13] J. Muhlemann, H. Maeda, C. Chang, P. Miguel, I. Baxter, B. Cooper, M. Perera, B. Nikolau, O. Vitek, J. Morgan, N. Dudareva, Developmental changes in the metabolic network of snapdragon flowers, PLoS One 7 (2012) e40381.
[14] R. Kakuda, M. Imai, Y. Yoita, K. Machida, M. Kikuchi, Secoiridoid glycosides from the flower buds of *Lonicera japonica*, Phytochemistry. 55 (2000) 879–881.
[15] B.H. Ter Kuile, H.V. Westerhoff, Transcriptome meets metabolome: hierarchical and metabolic regulation of the glycolytic pathway, FEBS Lett. 500 (2001) 169–171.
[16] U. Glaubitz, X. Li, S. Schaedel, A. Erban, R. Sulpice, J. Kopka, D.K. Hincha, E. Zuther, Integrated analysis of rice transcriptomic and metabolomic responses to elevated night temperatures identifies sensitivity-and tolerance-related profiles, Plant Cell Environ. 40 (2017) 121–137.
[17] P.E. Abraham, H. Yin, A.M. Borland, D. Weighill, S.D. Lim, H.C. De Paoli, N. Engle, P.C. Jones, R. Agh, D.J. Weston, S.D. Wullschleger, T. Tschaplinski, D. Jacobson, J.C. Cushman, R.L. Hettich, G.A. Tuskan, X. Yang, Transcript, protein and metabolite temporal dynamics in the CAM plant Agave, Nat. Plants. 2 (2016) 16178.
[18] U. Bechtold, C.A. Penfold, D.J. Jenkins, R. Legaie, J.D. Moore, T. Lawson, J.S. Matthews, S.R. Vialet-Chabrand, L. Baxter, S. Subramaniam, R. Hickman, H. Florance, C. Sambles, D.L. Salmon, R. Feil, L. Bowden, C. Hill, N.R. Baker, J.E. Lunn, B. Finkenstädt, A. Mead, V. Buchanan-Wollaston, J. Beynon, D.A. Rand, D.L. Wild, K.J. Denby, S. Ott, N. Smirnoff, P.M. Mullineaux, Time-series transcriptomics reveals that AGAMOUS-LIKE22 affects primary metabolism and developmental processes in drought-stressed *Arabidopsis*, Plant Cell 28 (2016) 345.
[19] H. Rischer, M. Oreώiᾰ, T. Seppänen-Laakso, M. Katajamaa, F. Lammertyn, W. Ardiles-Diaz, M.C. Van Montagu, D. Inzé, K.M. Oksman-Caldentey, A. Goossens, Gene-to-metabolite networks for terpenoid indole alkaloid biosynthesis in *Catharanthus roseus* cells, Proc. Natl. Acad. Sci. U. S. A. 103 (2006) 5614.
[20] T. Kim, K. Dreher, R. Nilo-Poyanco, I. Lee, O. Fiehn, B.M. Lange, B.J. Nikolau, L. Sumner, R. Welti, E.S. Wurtele, S.Y. Rhee, Patterns of metabolite changes identified from large-scale gene perturbations in *Arabidopsis* thaliana using a genome-scale metabolic network, Plant Physiol. 167 (2015) 1685–1698.
[21] P. Broun, Transcriptional control of flavonoid biosynthesis: a complex network of conserved regulators involved in multiple aspects of differentiation in *Arabidopsis*, Curr. Opin. Plant Biol. 8 (2005) 272–279.
[22] C.M. Fraser, C. Chapple, The phenylpropanoid pathway in *Arabidopsis*, *Arabidopsis* Book 9 (2011) e0152.

[23] Y. Yuan, Z. Wang, C. Jiang, X. Wang, L. Huang, Exploiting genes and functional diversity of chlorogenic acid and luteolin biosynthesis in *Lonicera japonica*, and their substitutes, Gene. 534 (2014) 408–416.
[24] S. Komatsu, C. Han, Y. Nanjo, M. Altaf-Un-Nahar, K. Wang, D. He, P. Yang, Label-free quantitative proteomic analysis of abscisic acid effect in early-stage soybean under flooding, J. Proteome Res. 12 (2013) 4769.
[25] M.M. Bradford, A rapid and sensitive method for the quantitation of microgram quantities of protein utilizing the principle of protein-dye binding, Anal. Biochem. 72 (1976) 248–254.
[26] Y. Nanjo, L. Skultety, L. Uváčková, K. Klubicová, M. Hajduch, S. Komatsu, Mass spectrometry-based analysis of proteomic changes in the root tips of flooded soybean seedlings, J. Proteome Res. 11 (2012) 372.
[27] J.V. Olsen, L.M.F. de Godoy, G. Li, B. Macek, P. Mortensen, R. Pesch, A. Makarov, O. Lange, S. Horning, M. Mann, Parts per million mass accuracy on an Orbitrap mass spectrometer via lock mass injection into a C-trap, Mol. Cell. Proteomics 4 (2005) 2010.
[28] M. Brosch, L. Yu, T. Hubbard, J. Choudhary, Accurate and sensitive peptide identification with mascot percolator, J. Proteome Res. 8 (2009) 3176–3181.
[29] K. Shinoda, M. Tomita, Y. Ishihama, emPAI Calc-for the estimation of protein abundance from large-scale identification data by liquid chromatography-tandem mass spectrometry, Bioinformatics. 26 (2010) 576–577.
[30] M.G. Grabherr, B.J. Haas, M. Yassour, J.Z. Levin, D.A. Thompson, I. Amit, X. Adiconis, L. Fan, R. Raychowdhury, Q. Zeng, Full-length transcriptome assembly from RNA-Seq data without a reference genome, Nat. Biotechnol. 29 (2011) 644–652.
[31] Y. Xiao, Y. Yang, H. Cao, H. Fan, Z. Ma, X. Lei, A.S. Mason, Z. Xia, X. Huang, Efficient isolation of high quality RNA from tropical palms for RNA-seq analysis, Plant Omics. 5 (2012) 584–589.
[32] C. Iseli, C.V. Jongeneel, P. Bucher, ESTScan: a program for detecting, evaluating, and reconstructing potential coding regions in EST sequences, Proc. Int. Conf. Intell. Syst. Mol. Biol. AAAI Press, Menlo Park, CA, 1999, pp. 138–148.
[33] B. Yang, Q. Guan, J. Tian, S. Komatsu, Transcriptomic and proteomic analyses of leaves from *Clematis terniflora* DC. Under high level of ultraviolet-B irradiation followed by dark treatment, J. Proteome 150 (2017) 323–340.
[34] B. Usadel, A. Nagel, O. Thimm, H. Redestig, O.E. Blaesing, N. Palacios-Rofas, J. Selbig, J. Hannemann, M.C. Piques, D. Steinhauser, W.R. Scheible, Y. Gibon, R. Morcuende, D. Weicht, S. Meyer, M. Stitt, Extension of the visualization tool MapMan to allow statistical analysis of arrays, display of corresponding genes, and comparison with known responses, Plant Physiol. 138 (2005) 1195–1204.
[35] M. Kanehisa, S. Goto, KEGG: kyoto encyclopaedia of genes and genomes, Nucleic Acids Res. 28 (2000) 27–30.
[36] R. Kolde, M.R. Kolde, Package 'Pheatmap'. R Package, vol. 1, (2015), p. 7.
[37] G.L. Müller, M.F. Drincovich, C.S. Andreo, M.V. Lara, Role of photosynthesis and analysis of key enzymes involved in primary metabolism throughout the lifespan of the tobacco flower, J. Exp. Bot. 61 (13) (2010) 3675–3688.
[38] J.K. Muhlemann, H. Maeda, C.Y. Chang, M.P. San, I. Baxter, B. Cooper, M.A. Perera, B.J. Nikolau, O. Vitek, J.A. Morgan, N. Dudareva, Developmental changes in the metabolic network of snapdragon flowers, PLoS One 7 (2012) 40381.
[39] C. Wagstaff, T.J.W. Yang, A.D. Stead, V. Buchanan-Wollaston, J.A. Roberts, A molecular and structural characterization of senescing *Arabidopsis* siliques and comparison of transcriptional profiles with senescing petals and leaves, Plant J. 57 (2010) 690–705.
[40] L.M. Galindo González, W. El Kayal, C.J. Ju, C.C. Allen, S. King-Jones, J.E. Cooke, Integrated transcriptomic and proteomic profiling of white spruce stems during the transition from active growth to dormancy, Plant Cell Environ. 35 (4) (2012) 682–701.
[41] M. Li, K. Wang, S. Li, P. Yang, Exploration of rice pistil responses during early post-pollination through a combined proteomic and transcriptomic analysis, J. Proteome 131 (2016) 214–226.
[42] O. Blokhina, E. Virolainen, K.V. Fagerstedt, Antioxidants, oxidative damage and oxygen deprivation stress: a review, Ann. Bot. 91 (2003) 179–194.
[43] M. McConn, J. Browse, The critical requirement for linolenic acid is pollen development, not photosynthesis, in an *Arabidopsis* mutant, Plant Cell 8 (1996) 403–416.
[44] E.E. Farmer, C.A. Ryan, Octadecanoid precursors of jasmonic acid activate the synthesis of wound-inducible proteinase inhibitors, Plant Cell 4 (1992) 129–134.
[45] X. Gao, Q. Yang, C. Minami, H. Matsuura, A. Kimura, T. Yoshihara, Inhibitory effect of salicylhydroxamic acid on theobroxide-induced potato tuber formation, Plant Sci. 165 (2003) 993–999.
[46] K.H. Nam, C. Minami, F. Kong, H. Matsuura, K. Takahashi, T. Yoshihara, Relation between environmental factors and the LOX activities upon potato tuber formation and flower-bud formation in morning glory, Plant Growth Regul. 46 (2005) 253–260.
[47] M. Yokoyama, S. Yamaguchi, S. Inomata, K. Komatsu, S. Yoshida, T. Iida, Y. Yokokawa, M. Yamaguchi, S. Kaihara, A. Takimoto, Stress-induced factor involved in flower formation of Lemna is an alpha-ketol derivative of linolenic acid, Plant Cell Physiol. 41 (2000) 110–113.
[48] W. Plaxton, The organization and regulation of plant glycolysis, Annu. Rev. Plant Physiol. Plant Mol. Biol. 47 (1996) 185–214.
[49] K. Herrmann, L. Weaver, The shikimate pathway, Annu. Rev. Plant Physiol. Plant Mol. Biol. 50 (1999) 473–503.
[50] M. Ohtani, K. Morisaki, Y. Sawada, R. Sano, A. Uy, A. Yamamoto, T. Kurata, Y. Nakano, S. Suzuki, M. Matsuda, T. Hasunuma, M. Hirai, T. Demura, Primary metabolism during biosynthesis of secondary wall polymers of protoxylem vessel elements, Plant Physiol. 172 (2016) 1612–1624.
[51] R. Julkunen-Tiitto, N. Nenadis, S. Neugart, M. Robson, G. Agati, J. Vepsäläinen, G. Zipoli, L. Nybakken, B. Winkler, M.A.K. Jansen, Assessing the response of plant flavonoids to UV radiation: an overview of appropriate techniques, Phytochem. Rev. 14 (2015) 273–297.
[52] M. Kusano, T. Tohge, A. Fukushima, M. Kobayashi, N. Hayashi, H. Otsuki, Y. Kondou, H. Goto, M. Kawashima, F. Matsuda, F. Niida, M. Matsui, K. Saito, A.R. Fernie, Metabolomics reveals comprehensive reprogramming involving two independent metabolic responses of *Arabidopsis* to UV-B light, Plant J. Cell Mol. Biol. 67 (2011) 354–369.
[53] R. Nakabayashi, K. Yonekura-Sakakibara, K. Urano, M. Suzuki, Y. Yamada, T. Nishizawa, F. Matsuda, M. Kojima, H. Sakakibara, K. Shinozaki, A.J. Michael, T. Tohge, M. Yamazaki, K. Saito, Enhancement of oxidative and drought tolerance in *Arabidopsis* by overaccumulation of antioxidant flavonoids, Plant J. 77 (2014) 367–379.
[54] G. Agati, E. Azzarello, S. Pollastri, M. Tattini, Flavonoids as antioxidants in plants: location and functional significance, Plant Sci. 196 (2012) 67–76.
[55] N. Dudareva, E. Pichersky, Metabolic engineering of plant volatiles, Curr. Opin. Biotechnol. 19 (2) (2008) 181–189.
[56] K.M. Herrmann, L.M. Weaver, The shikimate pathway: early steps in the biosynthesis of aromatic compounds, Plant Cell 7 (1995) 907–919.
[57] S. Henkes, U. Sonnewald, R. Badur, R. Flachmann, M. Stitt, A small decrease of plastid transketolase activity in antisense tobacco transformants has dramatic effects on photosynthesis and phenylpropanoid metabolism, Plant Cell 13 (2001) 535–551.
[58] M. Khozaei, S. Fisk, T. Lawson, Y. Gibon, R. Sulpice, M. Stitt, S.C. Lefebvre, C.A. Raines, Overexpression of plastid transketolase in tobacco results in a thiamine auxotrophic phenotype, Plant Cell 27 (2) (2015) 432–447.
[59] T. Mettler, T. Mühlhaus, D. Hemme, M.A. Schöttler, J. Rupprecht, A. Idoine, D. Veyel, S.K. Pal, L. Yaneva-Roder, F.V. Winck, F. Sommer, D. Vosloh, B. Seiwert, A. Erban, A. Burgos, S. Arvidsson, S. Schönfelder, A. Arnold, M. Günther, U. Krause, M. Lohse, J. Kopka, Z. Nikoloski, B. Mueller-Roeber, L. Willmitzer, R. Bock, M. Schroda, M. Stitt, Systems analysis of the response of photosynthesis, metabolism, and growth to an increase in irradiance in the photosynthetic model organism Chlamydomonas reinhardtii, Plant Cell 26 (2014) 2310–2350.
[60] M. Rapala-Kozik, N. Wolak, M. Kujda, A.K. Banas, The upregulation of thiamine (vitamin B1) biosynthesis in Arabidopsis thaliana seedlings under salt and osmotic stress conditions is mediated by abscisic acid at the early stages of this stress response, BMC Plant Biol. 12 (2012) 2.
[61] F. Bouvier, A. d'Harlingue, C. Suire, R.A. Backhaus, B. Camara, Dedicated roles of plastid transketolases during the early onset of isoprenoid biogenesis in pepper fruits1, Plant Physiol. 117 (4) (1998) 1423–1431.
[62] J. Estevez, A. Cantero, A. Reindl, S. Reichler, P. León, 1-Deoxy-D-xylulose-5-phosphate synthase, a limiting enzyme for plastidic isoprenoid biosynthesis in plants, J. Biol. Chem. 276 (2001) 22901–22909.
[63] Q. Qi, B. Trimming, K. Kleppinger-Sparace, M. Emes, S. Sparace, Pyruvate dehydrogenase complex and acetyl-CoA carboxylase in pea root plastids: their characterization and role in modulating glycolytic carbon flow to fatty acid biosynthesis, J. Exp. Bot. 47 (1996) 1889–1896.
[64] I. Oguni, I. Uritani, Effect of (−)-hydroxycitrate on ipomeamarone biosynthesis from pyruvate in sweet potato with black rot, Plant Cell Physiol. 15 (1974) 179–182.